



Generation of two human iPSC lines (HIMRi002-A and HIMRi003-A) derived from Caveolinopathy patients with rippling muscle disease

A. Boeing^{a,1}, L. Mavrommatis^{a,1}, N.M. Daya^a, H. Zhuge^a, L. Volke^a, A. Kocabas^a, M. Kneifel^a, M. Athamneh^a, K. Krause^a, N. Südkamp^a, K. Döring^b, C. Theiss^c, A. Roos^a, H. Zaehres^d, A.K. Güttches^a, M. Vorgerd^{a,*}

^a Department of Neurology, Heimer Institute for Muscle Research, BG-University Hospital Bergmannsheil, Ruhr-University Bochum, 44789 Bochum, Germany

^b Department of Human Genetics, Ruhr-University Bochum, 44801 Bochum, Germany

^c Department of Cytology, Ruhr-University Bochum, 44801 Bochum, Germany

^d Department of Anatomy and Molecular Embryology, Institute of Anatomy, Ruhr-University Bochum, 44801 Bochum, Germany

ABSTRACT

Here we introduce the human induced pluripotent stem cell lines (hiPSCs), HIMRi002-A and HIMRi003-A, generated from cultured dermal fibroblasts of 61-year-old (HIMRi002-A) and 38-year-old (HIMRi003-A) female patients, carrying a known heterozygous pathogenic variant (*p.A46T*) in the *Caveolin 3* (*CAV3*) gene, via lentiviral expression of OCT4, SOX2, KLF4 and c-MYC. HIMRi002-A and HIMRi003-A display typical embryonic stem cell-like morphology, carry the *p.A46T CAV3* gene mutation, express several pluripotent stem cell markers, retain normal karyotype (46, XX) and can differentiate in all three germ layers. We postulate that the HIMRi002-A and HIMRi003-A iPSC lines can be used for the characterization of *CAV3*-associated pathomechanisms and for developing new therapeutic options.

1. Resource Table

Unique stem cell lines identifier	HIMRi002-A, HIMRi003-A
Alternative name(s) of stem cell lines	<i>p.A46T CAV3</i> hiPSCs
Institution	Department of Neurology, Heimer Institute for Muscle Research, BG-University Hospital Bergmannsheil, Ruhr-University Bochum, 44,789 Bochum, Germany
Contact information of distributor	Matthias Vorgerd, matthias.vorgerd@bergmannsheil.de
Type of cell lines	iPSC
Origin	Human
Additional origin info required for human ESC or iPSC	HIMRi002-A HIMRi003-A Age: 61 38 Sex: Female Female Ethnicity if known: Caucasian Caucasian
Cell Source	Dermal Fibroblasts
Clonality	Clonal
Method of reprogramming	Lentiviral
Genetic Modification	No
Type of Genetic Modification	Congenital
Evidence of the reprogramming transgene loss (including genomic copy if applicable)	tdTomato negative colonies – silencing of the transgene <i>CMV promoter</i> .

(continued on next column)

(continued)

Associated disease	Caveolinopathy, Degenerative dominant myopathy
Gene/locus	<i>CAV3</i> / NC_000003.12
Date archived/stock date	2023–03
Cell line repository/bank	https://hpscereg.eu/search?q=HIMR
Ethical approval	Patient material was collected at the University Hospital Bergmannsheil after ethical approval from the ethics commission of the Ruhr-University Bochum, Medical Faculty (15–5401, 08/2015).

2. Resource utility

Different disease phenotypes including a subtype of an autosomal-dominant limb girdle muscular dystrophy and rippling muscle disease (RMD) are caused by pathogenic variants in *CAV3*. It is of utmost importance to further analyse the complex pathophysiology in *CAV3*-associated myopathies (defined as caveolinopathies) in validated *in vitro* systems. The HIMRi002-A and HIMRi003-A iPSC-lines were established from *p.A46T CAV3* patients derived dermal fibroblasts using a lentiviral delivery of OCT4, SOX2, KLF4 and c-MYC. These cells represent a

* Corresponding author.

E-mail address: matthias.vorgerd@bergmannsheil.de (M. Vorgerd).

¹ Contributed equally to authorship.

promising model for studying *CAV3*-associated pathomechanisms and potential treatment options.

3. Resource details

Muscle diseases caused by pathogenic *CAV3* variants are called caveolinopathies (Gazzerro et al., 2010). To date, more than 40 pathogenic *CAV3* variants, located at different *CAV3* protein domains, have been described, and are leading to a variety of disease phenotypes, including limb girdle muscular dystrophy (LGMD) with potential to induce cardiomyopathy, rippling muscle disease (RMD), distal myopathy (DM) and hyperCKemia (Gazzerro et al., 2010). Until recently, there is no report demonstrating a clear genotype-phenotype correlation, thus some of the phenotypes might be present as a clinical continuum (Vorgerd, et al., 2001; Fischer et al., 2003). However, dominant as well as recessive *CAV3* variants are commonly associated with lowered sarcolemmal *CAV3* levels, reduction of caveolae at the sarcolemma, alterations of the triads (T-Tubuli/ Sarcoplasmic reticulum) and accumulation of *CAV3*-aggregates within the Golgi system.

To establish an *in-vitro* high-throughput disease modelling for caveolinopathies, we obtained skin fibroblasts, by punch biopsy and under sterile conditions, from a 61-year-old female *CAV3* patient with muscle

weakness and generalized RMD symptoms (percussion-induced muscle contractions, rippling muscles, muscle mounding) and from a 38-year-old female patient with exercise-induced muscle weakness and generalized RMD symptoms. Both patients carry the pathogenic heterozygous amino acid substitution p.A46T within the *CAV3* protein (Betz et al., 2001). Dermal fibroblasts were transduced with a polycistronic lentiviral vector expressing OCT4, SOX2, KLF4 and c-MYC cDNAs to induce reprogramming for a 3–4-week period. Upon colony formation, putative iPSC colonies were mechanically dissociated and cultured independently for clonal propagation. hiPSCs clones from both patients, that exhibited the typical hiPSCs morphology and absence of transgene expression (Fig. 1A) underwent standard pluripotent characterisation. Moreover, Immunofluorescence analysis indicated that the HIMRi002-A and HIMRi003-A hiPSC lines expressed representative pluripotency markers, including OCT4, SSEA4, TRA-1-60 and SOX2 (Fig. 1C). Furthermore, quantitative qPCR analysis indicated that in comparison to dermal fibroblasts expression levels, endogenous expression of OCT4, NANOG, and SOX2 were significantly upregulated in both iPSC lines, while in comparison to the published CB CD34⁺ derived hiPSC line (Dorn et al., 2015) exhibited similar expression levels (Fig. 1B). Karyotype high-throughput analysis via B-allele frequency and LogR ratio demonstrated no chromosomal aberrations associated with

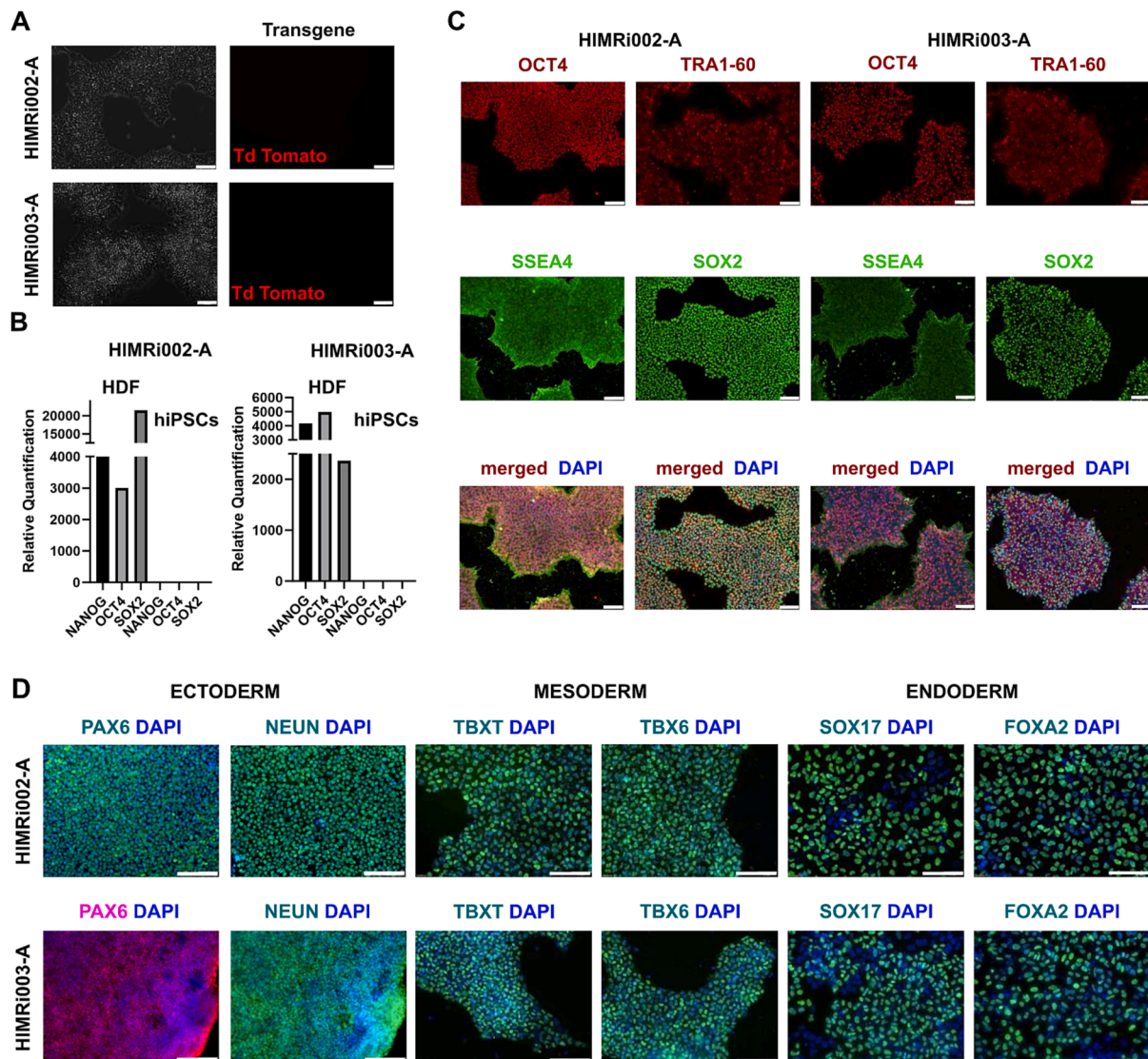


Fig. 1. Characterization of HIMRi002-A and HIMRi003-A hiPSC lines (HDF: Human Dermal Fibroblasts, hiPSCs: Control CB CD34⁺ derived hiPSCs, Dorn et al., 2015, Scale Bars: 100 μ M).

reprogramming in the HIMRi002-A and HIMRi003-A iPSC lines ([Supplementary Data](#)). During three-lineage directed differentiation assay both hiPSCs lines successfully gave rise to populations of all three embryonic germ layers ectoderm, mesoderm, and endoderm ([Fig. 1D](#)). Overall, the HIMRi002-A and HIMRi003-A iPSC lines fulfilled all the hallmarks of pluripotency.

4. Materials and methods

4.1. Virus production

HEKT293 cells (ATCC) were transfected with plasmid vectors, psPAX2 (Addgene, #12260), pMD2.G (Addgene, #12259) and pRRL.PPT.SF.hOct34.hKlf4.hSox2.hMyc.i2dTomato.pre ([Warlich et al., 2011](#), kindly provided by Prof. Schambach, MHH Hannover) at a 3:2:1 ratio using the FuGENE® HD Transfection Reagent (Promega). 48 hr post-transfection, the supernatant containing the lentivirus was collected, filtered through a 0.4-µm PVDF filter (Millipore) to remove any residual cell debris and concentrated via centrifugation (3000 rpm, 4 °C) using the Vivaspin® 20 Ultrafiltration unit (50,000 MWCO, PES, Santorius #VS2032). Lentiviral concentrate was suspended in DMEM (PAN Biotech) at a 10x fold of the initial supernatant volume and stored at -802 °C.

4.2. Cellular reprogramming

30.000 cells*cm⁻² of the CAV3 p.A46T dermal fibroblasts (BG-University Hospital Bergmannsheil - Heimer Institute for Muscle Research, passage #5) were plated on Matrigel®-coated six-well plate (Corning®). The next day, cells were infected with lentivirus expressing the OCT4, SOX2, KLF4 and c-MYC cDNAs in the presence of 6 µg/ml polybrene transfection reagent (Merck, #TR-1003-G) over the course of two days. Following viral infection, cells were washed once with PBS and cultured in fibroblast medium. Three days post infection, cell culture medium was switched to 1:1 ratio of fibroblast/ hiPSCs maintenance medium (StemFlex™, ThermoFisher Scientific, # A3349401). At day 5 post infection, cell culture medium was switched completely to hiPSCs maintenance medium. Between 21 and 28 days post viral infection, putative hiPSCs colonies were mechanically isolated, re-plated onto Matrigel®-coated plates and cultured in hiPSCs maintenance medium. The medium was refreshed daily, and hiPSCs upon 70–80 % confluency, were passaged using chemical dissociation (TrypLE™ Express, ThermoFisher Scientific). To validate transgene silencing, since the reprogramming cassette was conjugated to tdTomato (ORF), absence of tdTomato on hiPSCs indicated endogenous gene expression of the pluripotency markers and silencing of the lentiviral expression cassette during reprogramming. The cells were cultured at 37 °C, 90 % humidity and 5 % CO₂ ([Table 1](#)).

4.3. Quantitative PCR-analysis

Total RNA isolation was performed using the Quick-RNA™ MiniPrep kit (ZYMO RESEARCH), followed by reverse transcription and cDNA synthesis using the High Capacity cDNA Reverse Transcription Kit (Applied Biosystem™-ThermoFisher Scientific) according to the manufacturer's instructions. qPCR was performed using iTaq™ Universal SYBR® Green Supermix (Bio-Rad). RT-qPCR was performed using iTaq™ Universal SYBR® Green Supermix (Bio-Rad). Relative gene expression levels were calculated by the 2^{-ΔΔCt} method, normalized to an endogenous control gene and presented as fold change over the p.A46T CAV3 dermal fibroblasts and to control CB CD34⁺ derived hiPSCs ([Dorn et al., 2015](#)). Primers are listed in [Table 2](#).

4.4. Microarray karyotyping

Genomic DNA from all cell lines was extracted using the Quick-DNA

Table 1
Characterization and validation.

Classification	Test	Result	Data
Morphology Phenotype	Brightfield Image	normal	Fig. 1 A
	Qualitative analysis	Positive for OCT3/4,	Fig. 1 C
	Immunocytochemistry	SOX2, TRA 1–60, SSEA-4	
Genotype	Quantitative analysis RT-qPCR	Positive for NANOG, OCT4, SOX2, relatively to the dermal fibroblasts	Fig. 1 B
	Karyotype (Infinium Assay Data for Whole-Genome Structural Variation)	46 XX	Fig. 1 E
Identity	STR analysis	N/A 16 sites tested (15 STR loci and Amelogenin), and all matched	N/A Supplementary Data
	Sequencing	heterozygous	Betz et al., 2001
Mutation analysis (IF APPLICABLE)	Southern Blot OR WGS	N/A	N/A
	Microbiology and virology	Mycoplasma testing by MycoAlert mycoplasma detection kit. Negative	Supplementary Data
Differentiation potential	Directed differentiation	Ectoderm Mesoderm Endoderm	Fig. 1 D
List of recommended germ layer markers	Expression of these markers has to be demonstrated at mRNA (RT PCR) or protein (IF) levels, at least 2 markers need to be shown per germ layer	Ectoderm: PAX6, NeuN Endoderm: SOX17, FOXA2 Mesoderm: BRACHYURY/ TBXT, TBX6,	Fig. 1 D
Donor screening (OPTIONAL)	HIV 1 + 2 Hepatitis B, Hepatitis C	N/A	N/A
Genotype additional info (OPTIONAL)	Blood group genotyping	N/A	N/A
	HLA tissue typing	N/A	N/A

kit (ZymoResearch). High-throughput genotyping was performed via Illumina® iScan technology (Bonn Life & Brain Genomics, University of Bonn) and karyograms were generated using the GenomeStudio 2.0 software too (Illumina).

4.5. Differentiation assay

The pluripotent potential of HIMRi002-A (passage #6) and HIMRi003-A (passage #5) hiPSCs was further validated via three-lineage directed differentiation assay (STEMdiff™ Trilineage Differentiation Kit, STEMCELL™ Technologies, #05230) according to the manufacturer's instructions.

4.6. Short tandem repeat (STR) analysis

Genomic DNA was isolated from the fibroblasts (passage #8) and HIMRi002-A (passage #6) and HIMRi003-A (passage #4) iPSCs lines using the Quick-DNA kit (ZymoResearch) STR analysis was performed via the PowerPlex 16 system (Promega) according to the manufacturer's instructions. Obtained fragments were run on a 3500XL Genetic Analyzer instrument (Applied Biosystems) and analysed via the GeneMapper Software 5 (Applied Biosystems) ([Supplementary Data](#)).

Table 2
Reagents details.

	Antibodies used for immunocytochemistry/flow-cytometry			
	Antibody	Dilution	Company Cat #	RRID
Pluripotency Markers	Pluripotent Stem Cell 4-Marker Immunocytochemistry Kit:			
	Rabbit Anti-Human OCT4	1:200	Invitrogen™ #A24881	RRID: AB_2650999
	Rat Anti-Human SOX2	1:100		
	Mouse Anti-Human SSEA4	1:100		
Differentiation Markers	Mouse Anti-Human TRA-1-60	1:100		
	Mouse anti-PAX6	1:200	DHSB: # pax6	RRID: AB_528427
	Rabbit anti-NEUN	1:200	Abcam: # ab177487	RRID: AB_2532109
	Goat anti-BRACHYURY/TBXT	1:200	R&D Systems: # AF2085	RRID: AB_2200235
	Goat anti-TBX6	1:200	R&D Systems: # AF4744	RRID: AB_2200834
	Goat anti-SOX17	1:200	R&D Systems: # AF1924	RRID: AB_355060
Secondary antibodies	Goat anti- Human HNF-3 beta/FoxA2	1:200	R&D Systems: # AF2400	RRID: AB_2294104
	Pluripotent Stem Cell 4-Marker Immunocytochemistry Kit			
	Alexa Fluor 594 Donkey Anti-Rabbit	1:500	Invitrogen™ #A24881	RRID: AB_2650999
	Alexa Fluor 488 Donkey Anti-Rat	1:500		
	Alexa Fluor 594 Goat Anti-Mouse IgM	1:500		
	Alexa Fluor 488 Goat Anti-Mouse IgG3	1:500		
	Alexa Fluor 488 Donkey Anti-rabbit	1:1000	Invitrogen™ #A21206	RRID: AB_2535792
	Alexa Fluor 488 Donkey Anti-goat	1:1000	Invitrogen™ #A10037	RRID: AB_2534013
	Alexa Fluor 568 Donkey Anti-mouse	1:1000	Invitrogen™ #A11055	RRID: AB_2534102
	Primers			
	Target	Size of band	Forward/Reverse primer (5'-3')	
Pluripotency Markers (qPCR)	NANOG	116 bp	TTTGTGGCCTGAAGAAAACCT/ AGGGCTGTCTGTAATAAGCAG	
	OCT4	156 bp	GTGTCAGCCAAAAGACCATCT/ GGCCTGCATGAGGGTTTGT	
	SOX2	215 bp	TGGACAGTTACGCGCACAT/ CGAGTAGGACATGTCTGTAGGT	
House-Keeping Genes (qPCR)	GAPDH	101 bp	ACAACCTTGGTATCGTGAAGG/ GCCATCAGCCACAGTTTC	
	Caveolin 3	N/A	Betz et al., 2001	
Genotyping	N/A	N/A	N/A	
Targeted mutation analysis/sequencing	N/A	N/A	N/A	

4.7. Immunofluorescence

The pluripotent potential of HIMRi002-A (passage #4) and HIMRi003-A (passage #3) hiPSCs was verified using the commercially available Pluripotent Stem Cell 4-Marker Immunocytochemistry Kit (Invitrogen™, # A24881). During three-lineage and hiPSCs characterisation, cells were fixed with 4 % paraformaldehyde (PFA; Sigma-Aldrich) for 15 min at RT, permeabilised with 0.5 % Triton™ X-100 (Sigma-Aldrich) for 15 min and blocked with 5 % BSA (Carl ROTH®) for 1 h. Overnight primary antibody incubation at 4 °C, followed by 1h incubation with secondary antibodies at RT and mounted with ROTI®Mount FluorCare DAPI (Carl ROTH®, #HP20.1). In-between each step, cells washed three times with PBS. Images were acquired using the Olympus IX83 fluorescent inverted microscope, with the light source U-HGLGPS (OLYMPUS) and analysed with the cellSens software and ImageJ. Antibodies are listed in Table 2.

4.8. Mycoplasma test

MycAlert mycoplasma detection kit (Lonza) was used to exclude mycoplasma contamination.

Declaration of Competing Interest

The authors declare that they have no known competing financial interests or personal relationships that could have appeared to influence the work reported in this paper.

Acknowledgement

We thank Professor Axel Schambach, MHH Hannover for providing

the SF-OSKM reprogramming vector. We acknowledge support by the DFG Open Access Publication Funds of the Ruhr-University Bochum.

Appendix A. Supplementary data

Supplementary data to this article can be found online at <https://doi.org/10.1016/j.scr.2023.103220>.

References

- Betz, R.C., Schoser, B.G., Kasper, D., Ricker, K., Ramirez, A., Stein, V., Torbergson, T., Lee, Y.A., Nöthen, M.M., Wienker, T.F., Malin, J.P., Propping, P., Reis, A., Mortier, W., Jentsch, T.J., Vorgerd, M., Kubisch, C., 2001. Mutations in CAV3 cause mechanical hyperirritability of skeletal muscle in rippling muscle disease. *Nat. Genet.* 28 (3), 218–219. <https://doi.org/10.1038/90050>.
- Dorn, I., Klich, K., Arauzo-Bravo, M.J., Radstaak, M., Santourlidis, S., Ghanjati, F., Radke, T.F., Psathaki, O.E., Hargus, G., Kramer, J., Einhaus, M., Kim, J.B., Kögler, G., Wernet, P., Schöler, H.R., Schlenke, P., Zaehres, H., 2015. Erythroid differentiation of human induced pluripotent stem cells is independent of donor cell type of origin. *Haematologica* 100 (1), 32–41. <https://doi.org/10.3324/haematol.2014.108068>.
- Fischer, D., Schroers, A., Blümcke, I., Urbach, H., Zerres, K., Mortier, W., Vorgerd, M., Schröder, R., 2003. Consequences of a novel caveolin-3 mutation in a large German family. *Ann. Neurol.* 53 (2), 233–241. <https://doi.org/10.1002/ana.10442>.
- Gazzerro, E., Sotgia, F., Bruno, C., Lisanti, M.P., Minetti, C., 2010. Caveolinopathies: from the biology of caveolin-3 to human diseases. *Eur. J. Human Genet.* EJHG 18 (2), 137–145. <https://doi.org/10.1038/ejhg.2009.103>.
- Vorgerd, M., Ricker, K., Ziemssen, F., Kress, W., Goebel, H.H., Nix, W.A., Kubisch, C., Schoser, B.G., Mortier, W., 2001. A sporadic case of rippling muscle disease caused by a de novo caveolin-3 mutation. *Neurology* 57 (12), 2273–2277. <https://doi.org/10.1212/wnl.57.12.2273>.
- Warlich, E., Kuehle, J., Cantz, T., Brugman, M.H., Maetzig, T., Galla, M., Filipczyk, A.A., Halle, S., Klump, H., Schöler, H.R., Baum, C., Schroeder, T., Schambach, A., 2011. Lentiviral vector design and imaging approaches to visualize the early stages of cellular reprogramming. *Mol. Therapy* 19, 782–789. <https://doi.org/10.1038/mt.2010.314>.